Electronic Supplementary Material (ESI) for Journal of Materials Chemistry C.

Perylene diimide derivative via ionic self-assembly: helical supramolecular structure and selective detection of ATP

Lin Lu,[a,1] Hai-Jun Sun,[a,1] Yu-Ting Zeng,[a] Yu Shao,[b] Maxim V. Bermeshev,[c] Yang Zhao,[a] Bin Sun,*[,b] Zhi-Jian Chen,[a] Xiang-Kui Ren*[,a] and Meifang Zhu*[,b]

[a] School of Chemical Engineering and Technology, Tianjin University, Tianjin 300350, P. R. China

[b] State Key Laboratory for Modification of Chemical Fibers and Polymer Materials, College of Materials Science and Engineering, Donghua University, Shanghai 201620, P. R. China

[c] A.V. Topchiev Institute of Petrochemical Synthesis Russian Academy of Sciences, Moscow, 119991, Russia

E-mail: renxiangkui@tju.edu.cn, zmf@dhu.edu.cn, sunbin@dhu.edu.cn

[1] Lin Lu and Hai-Jun Sun contributed equally to this work.

Section 1. Structure Calculation Method

According to the principles of the reciprocal lattice and diffraction geometry shown in Figure 5, the *a**- and *b**-axes can be tentatively assumed to be on the equator, and the c*-axis is along the meridian, so the crystal structure is either orthorhombic or monoclinic. The crystal unit cell determination procedure was based on construction of the reciprocal lattice. Firstly, the (hk0) reciprocal lattice net, namely, a parallelogram with edges *a** and *b**, can be constructed by the values determined from the equatorial diffractions. The γ^* angle can be obtained when all of the (hk0) diffractions can be indexed based on the 2D *a***b** lattice. Afterwards, the *c** value can be determined from the meridianal diffractions, and then the quadrant diffractions can be indexed by the unit cell dimensions. Finally, computer refinement is conducted to achieve the fit with the least error between experimental results and calculated data. In this case, the six parameters of the unit cell dimensions (*a*, *b*, *c*, and α, β, γ) are obtained.

Section 2. Experimental Results

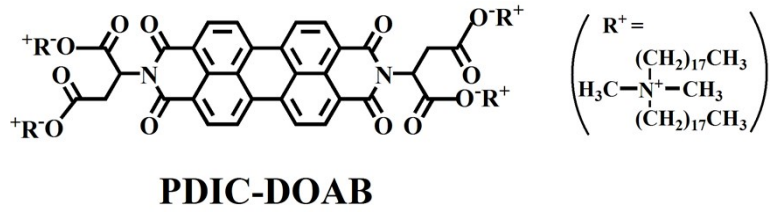

Fig. S1. Chemical structure of PDIC-DOAB.

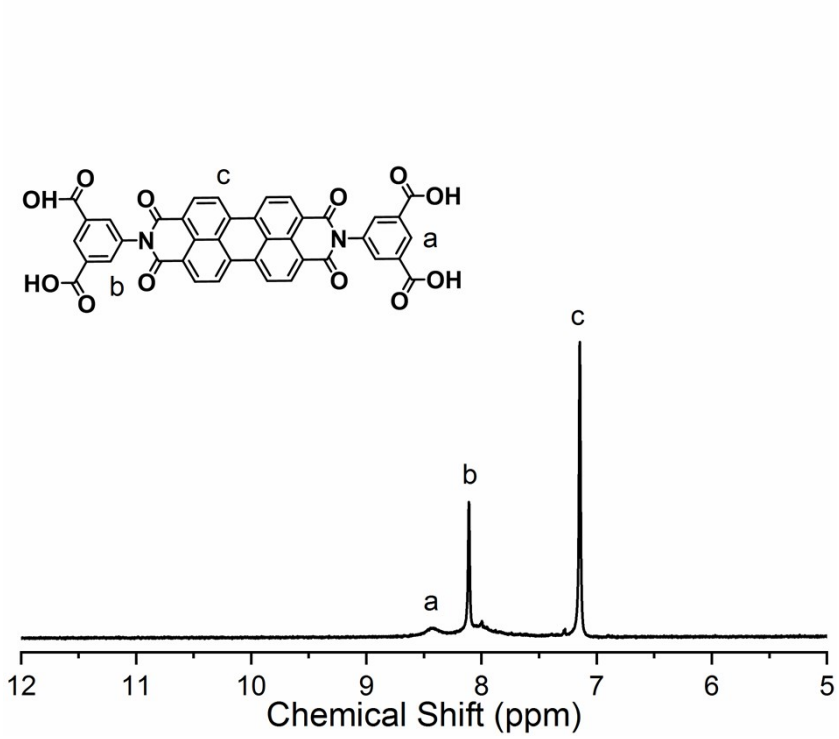

Fig. S2. ^{1}H NMR spectrum of PDTA (D_2O as solvent).

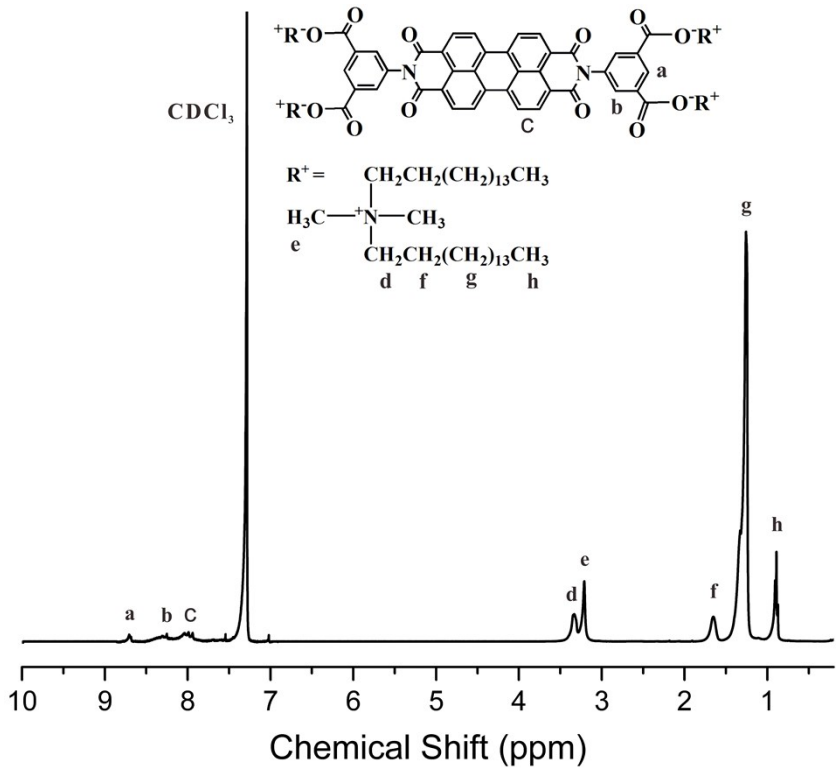

Fig. S3. ^{1}H NMR spectrum of PDTA-DHAB ($CDCl_3$ as solvent).

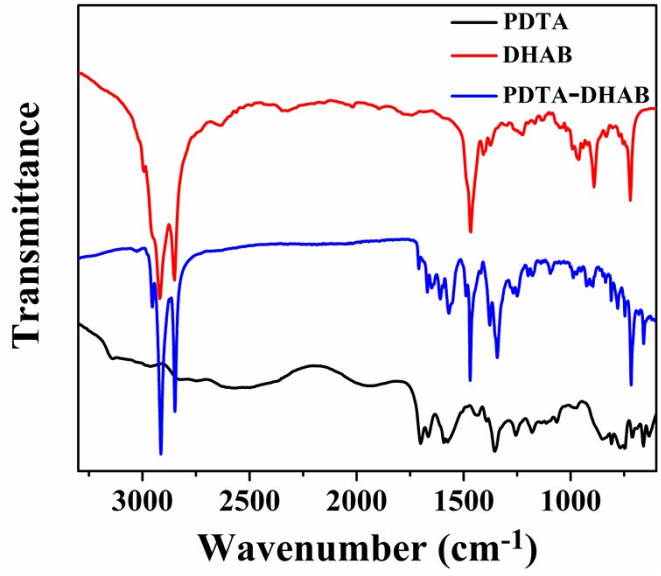

Fig. S4. FT-IR spectra of PDTA, DHAB and PDTA-DHAB.

Table S1. Concentration dependence of $A_{0\text{-}0}/A_{0\text{-}1}$ absorption ratios of PDTA-DHAB in different solvents.

$A_{0\text{-}0}/A_{0\text{-}1}$ [M]	CH_2Cl_2	Toluene
1×10^{-5}	1.50	1.05
2×10^{-5}	1.48	0.98
3×10^{-5}	1.46	0.96

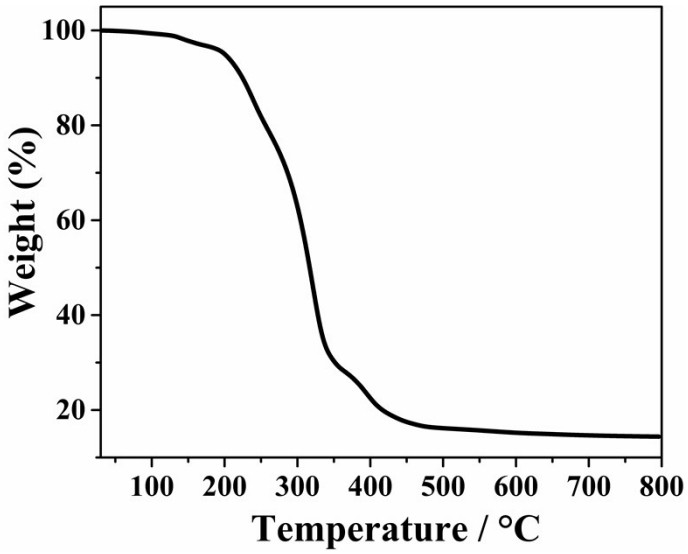

Fig. S5. TGA curve of the PDTA-DHAB complex.

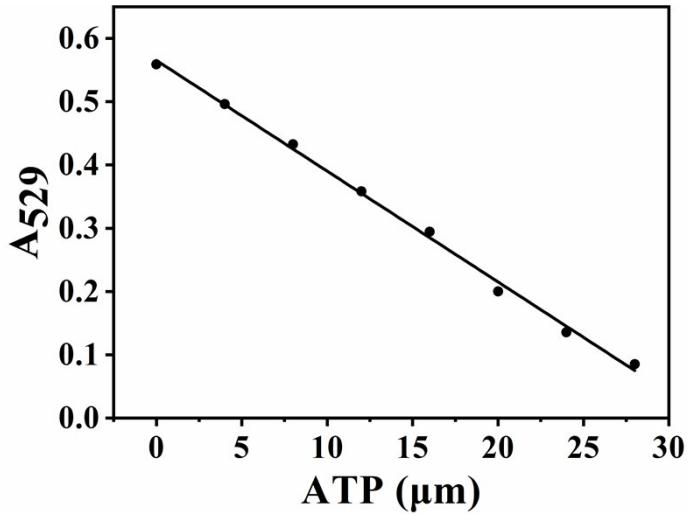

Fig. S6. Linear relationship between absorbance and ATP concentration of PDTA-DHAB at 529 nm.

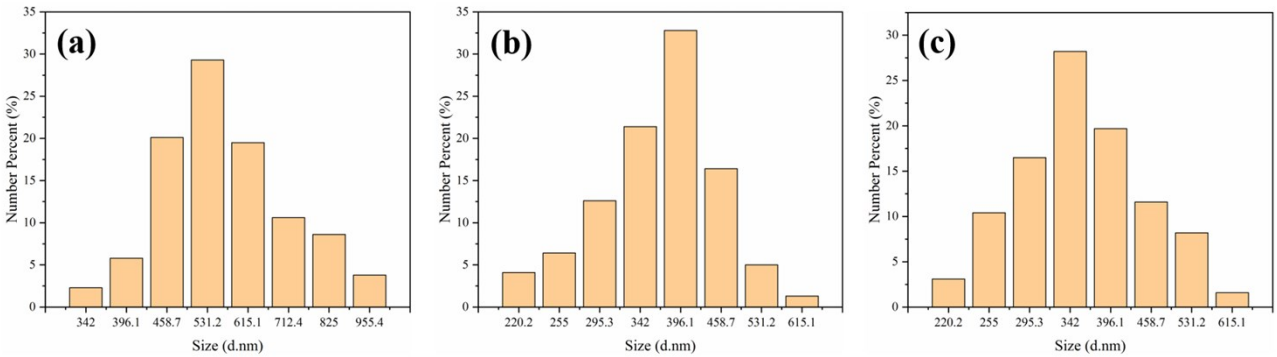

Fig. S7. Particle size distribution of PDTA-DHAB (10 μM) in the EtOH: H_2O (1:1) solution (a) upon the addition of ADP (4 equiv.). (b) upon the addition of AMP (4 equiv.). (c) upon the addition of Br^- (4 equiv.).

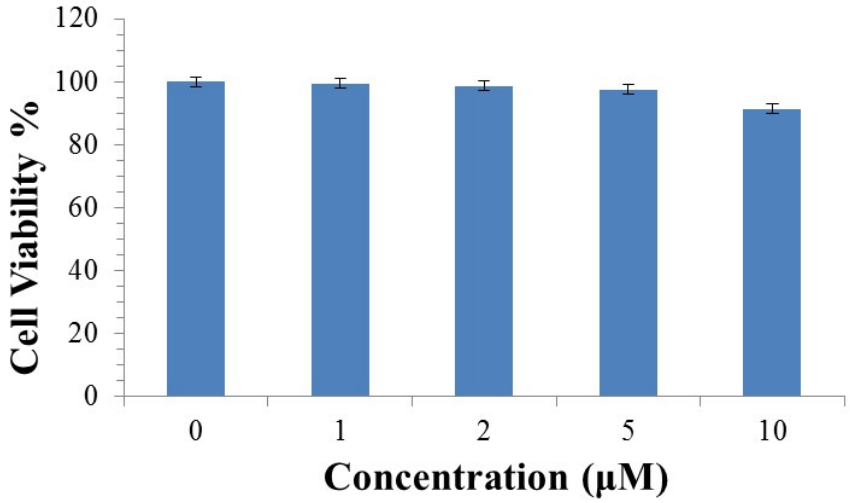

Fig. S8. HeLa cells were incubated with each concentration of PDTA-DHAB for 24 h. Cell viability was assayed by MTT test. Results are expressed as mean ± standard deviation of three independent experiments.